Film Riding Pressure Activated Leaf Seal Proof of Concept

Tracey Kirk[1], Aaron Bowsher[2], Peter Crudgington[3] & Andrew Pawlak[4]
Cross Manufacturing Co. (1938) Ltd, Devizes,Wiltshire,SN10 2EU, UK

Clayton Grondahl[5]
CMG Tech LLC, Rexford,New York, 12148, US

and

James Dudley[6]
Cincinnati, Ohio, 45249, US

The power generation expectation for turbine efficiency, service intervals and life continues to rise in order to meet stringent future targets. Sealing the gap between rotating and non-rotating parts, while accommodating the thermal growth, misalignment and rotor dynamics, is essential. Contacting seals show deterioration in sealing efficiency over time providing a potential advantage for use of film riding, non contact seals.

This paper presents initial test data for the Film Riding Pressure Activated Leaf Seal (FRPALS) for proof of concept. Testing has been completed using a custom designed test rig with large scale, 2-dimensional, linear sealing segments. The pressure profile and gap under the runner is examined and reported with comparison to theoretical performance at the design cold clearance of .120”. Further testing was conducted with cold build clearances either side of the design point for wider understanding of the activation behaviour.

Nomenclature

CFD	=	Computational Fluid Dynamics
FEM	=	Finite Element Modeling
FRPALS	=	Film Riding Pressure Activated Leaf Seal
FSD	=	Full Scale Deflection
g	=	Gauge
PALS	=	Pressure Activated Leaf Seal
PSI	=	Pounds per Square Inch

[1] Test & Dev, Brush Seals & Aerospace Products, Cross Mnfg Co. (1938) Ltd, Devizes, Wiltshire, SN10 2EU, UK
[2] Engineering Manger, Brush Seals & Aerospace Products, Cross Mnfg Co. (1938) Ltd, Devizes, Wiltshire, SN10 2EU, UK, AIAA Senior Member
[3] Director, Cross Mnfg Co. (1938) Ltd, Devizes, Wiltshire, SN10 2EU, UK, AIAA Senior Member
[4] Senior Technician, Cross Mnfg Co. (1938) Ltd, Devizes, Wiltshire, SN10 2EU, UK
[5] Director, CMG TECH LLC, 29 Stony Brook Drive, Rexford, New York, 12148
[6] Aircraft Engine Design Consultant, 11444 Brittany Woods Lane, Cincinnati, Ohio, 45249

I. Introduction

Shaft sealing is essential for efficiency and performance in turbomachinery. The expectation of the industry for longer service intervals and reduced degradation of power output due to wearing parts has lead to advancements in non-contacting and compliant sealing technology. Reduced efficiency due to shaft sealing over the life of a turbine is a result of multiple variations such as thermal distortion, misalignment, manufacturing tolerances and transient excursions [1]. Although contacting, compliant seals, such as brush seals, are proven technology with effective running of up to 100,000 hours in certain applications. They are not appropriate for all locations within a turbine and can be susceptible to wear due to large radial rotor-stator excursions. While traditional non-contacting solutions, such as labyrinth teeth, are designed with large radial clearances resulting in potentially high leakage at steady state operating conditions [2].

Non-contacting compliant seals [3, 4, 5, 6] rely on a balance of forces within their specific design to move radially during transient conditions maintaining a sufficient clearance between the rotor and seal without contact for the range of conditions within the application.

Advancing from the PALS concept [7], the evolution to the FRPALS was first introduced in 2010 [1] (Figure 1). This hydrostatic compliant seal uses the PALS concept of deflecting leaves that actuate under pressure loading to close down to the rotor under the desired operating conditions, while maintaining a large clearance at start/stop conditions. The concept is made up of several components that are designed to work under conditions required to meet application requirements. Initially the seal has a large radial clearance to the runner in cold conditions. As a pressure drop is applied across the seal, the force acting on the leaf elements results in a radial closure towards the rotor, until the balanced film forces under the runner generated by the Rayleigh step result in the film riding seal. The leaves and runners are designed to ensure the seal closure can accommodate start/stop conditions of the turbine as well as operate with a small clearance to the shaft at base load conditions. The seal is designed to avoid contact with the shaft in the turbines predicted operating cycle.

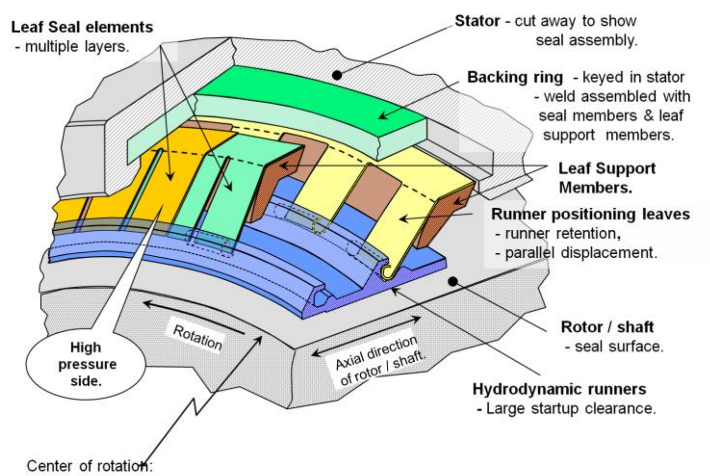

Figure 1: Film Riding Leaf Seal Concept [1]

II. Preliminary Development

Confirmation of runner film forces either by CFD analysis or physical testing was deemed essential to confidently design a proof of concept FRPALS. Analytical modeling by CFD analysis was considered but seen to be time-consuming and expensive compared to simplified bench testing that could offer quick solutions and validate results of subsequent models. Using an adaptation of CMG Tech's 2D test rig (Figure 2), initially built for the evaluation of the PALS segments, it was possible to quickly acquire physical pressure distribution data on the effects of various runner configurations.

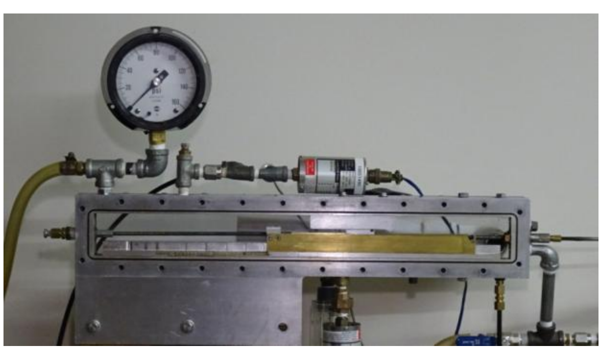

Figure 2: CMG Tech Bench Test Overview

Multiple tests were undertaken to optimize runner geometry for the Rayleigh step including axial step length, radial step height, radial gap and the ratio of step length to overall runner length. This was achieved by creating runner blocks segments of desired geometry for each test. The runner block segments were mounted on tapered rails in the test rig to accommodate testing at small increments of clearance relative to the base plate (i.e. effectively the rotor). Horizontally the runner segments were positioned in relation to a small diameter pressure tap in the base plate and when pressure was applied, translated axially against a lead screw. Slowly traversing the full axial length of the runner, a pressure transducer connected to the single pressure tap acquired the complete pressure profile under the runner (Figure 3). Runner pressure profile data was then processed to resolve runner force and center of pressure as a function of runner clearance for use in the analytical design in the next section. Runner geometry for the full scale proof of concept was based on these physical bench test results. The film force characteristics from the bench tests were used in the FEM model and the very good agreement between the performance predicted by the FEM model and the performance observed in tests provides confirmation that the bench test results were accurate.

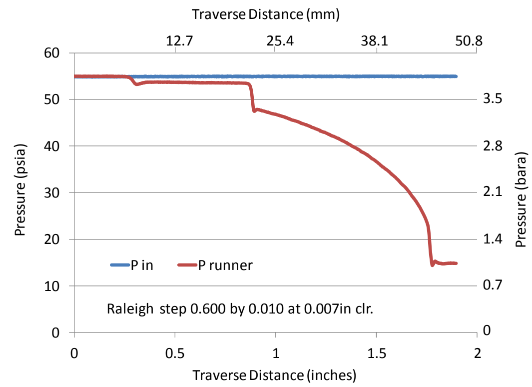

Figure 3: Runner Block Pressure Profile

III. Analytical Design

Specifications are established at the beginning of a design process including how much rotor eccentricity the seal is required to accommodate. This could be due to thermal distortion of the stator moving the seal relative to the centerline of the bearings, seal misalignment and run-out, or rotor radial motion within the bearings. These specifications established how much the runners need to travel radially while preserving a positive clearance with the rotor. The working pressure both upstream and downstream of the seal must be specified as well as the fluid temperature and viscosity.

A new design started with an estimation of each seal parameter based on experience from designing other FRPALS for similar applications. If the runner configuration is expected to be different from prior experience detailed CFD modeling and/or testing is needed to establish the film force characteristics for that runner configuration.

FEM then used the film force data from the CFD or bench testing to determine how closely that version fulfilled the specifications. Systematic variation of parameters and new FEM analyses were used to refine the concept design that fulfills all specifications and gave the smallest clearance between the seal runner and the rotor at the nominal operating conditions to provide the lowest leakage (Figure 4). Plotting clearance between the runner and the rotor for a range of runner eccentricity was helpful in comparing the performance of seal designs during the systematic variation of parameters to determine the best design. To obtain such a plot, the FEM analysis was not just a single point analysis, but the radial distance between the rotor and the seal housing was varied smoothly in a transient analysis while holding the upstream and downstream pressures constant at specified values. This gave a good view of how the seal behaved and supported selecting a set of design parameters to meet all requirements and maintain a minimum leakage (tightest runner/rotor clearance) at nominal operating conditions while avoiding a rotor rub at maximum eccentricity. Typical design parameters varied in this process were the seal leaf length, seal leaf thickness, knee angle of the leaf (angle between the leaf as assembled and a line parallel with the axis of the rotor), radius of curvature of the support which the leaf wraps around as pressure is applied, distance axially between the two sets of leaves supporting the runner, runner axial length and axial distance to the step.

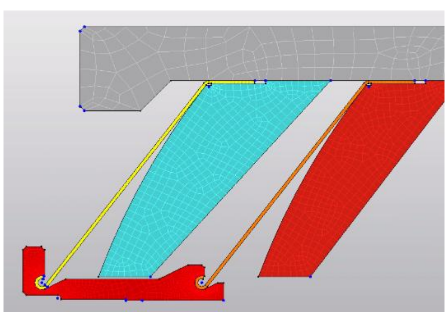

Figure 4: Early Concept FEM Model

IV. Large Application Scale Static Testing

A custom test rig was designed and built by Cross Manufacturing (Figure 5) utilizing air delivery system and data acquisition capabilities [8]. The test rig composed of a base for air to be fed into a chamber housing 3 segments of the FRPALS before venting to atmospheric conditions (Figure 6). The segments were mounted to a vertically adjustable top plate to investigate the effects of build eccentricity (Figure 7). Finally a static base plate was instrumented with 14 static pressure transducers and 4 proximity probes (Figure 8) to record the pressure distribution as the flow passed under the central runner and monitor the gap to ensure complete film riding. A viewing window was utilized to capture images of the closing event using high speed photography. The FRPALS segments were designed using a combination of bench test results and analytical approach to have the following geometry:

- Runner axial length – 1.500” [38.1mm]
- Rayleigh step height – 0.010” [0.25mm]
- Rayleigh step axial distance – 0.600” [15.24mm]
- Leaf thickness – 0.028” [0.71mm]
- Leaf length – 2.375” [60.33mm]
- Leaf angle – 52 degrees [0.908rad]
- Radius of curvature of the support – 6.600”[167.64mm]

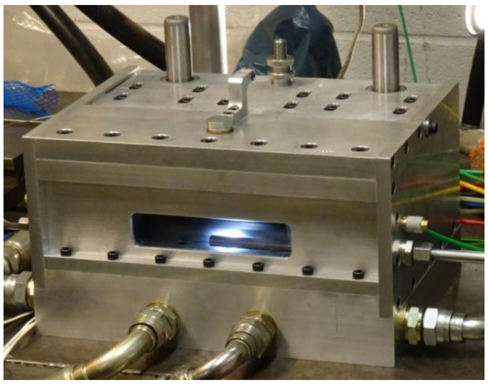

Figure 5: Overview of Static Test Rig

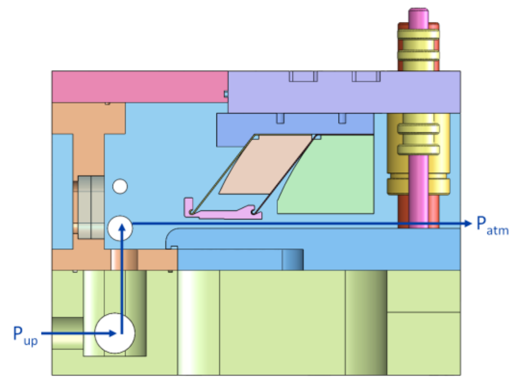

Figure 6: Model of Air Flow Path

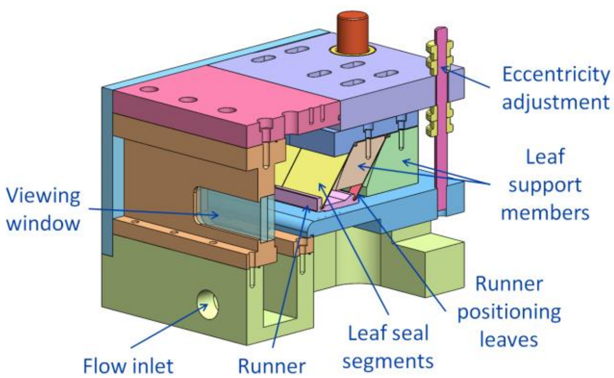

Figure 7: Model Cross Section of Static Test Rig

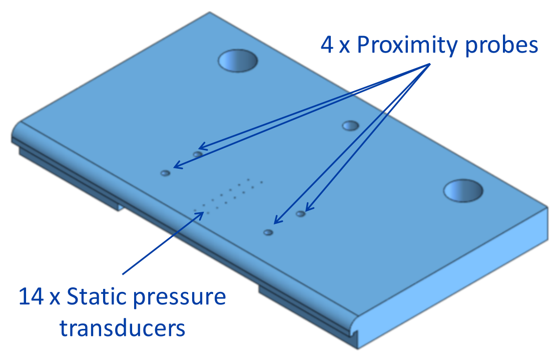

Figure 8: Instrumentation Locations in Base Plate

Four Capacitec HPT-40 proximity probes were threaded into the base plate with a range of 0.050” [1.27mm] and calibrated in position to within ±0.5% of full scale FSD. The sensors were set just below the surface ensuring that a reading would be achieved if the shoe contacted the base plate in operation. The purpose of the proximity probes was to monitor the film gap once the leaves had closed and compare each corner for tilt and rock (Figure 9 and Figure 10). It was not intended to monitor the closure event as the range of movement was greater than the proximity probes and the feasibility testing utilized low speed data acquisition for data points every 2 seconds.

Fourteen Druck 810 series static pressure transducers were also threaded into the base plate with various static pressure ranges depending on their location and calibrated within ±0.2% FSD. The transducers measured the static pressure at locations spanning the full length of the runner including the clearance step, Rayleigh step and the film riding area (Figure 9 & Figure 10)

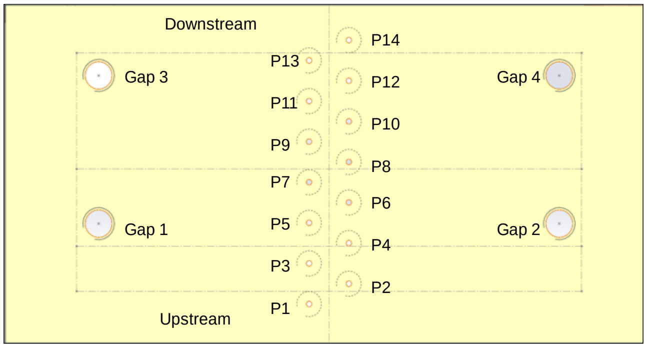

Figure 9: Schematic of Instrumentation Locations on the Base Plate Relative to the Runner

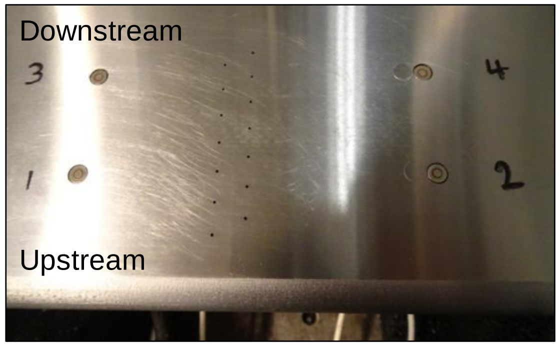

Figure 10: Instrumentation on Actual Base Plate

The test procedure began by setting the radial distance between the runner at cold conditions and the base plate to 0.120" [3.05mm]. This is the optimum design condition calculated using the analytical approach for this design and is referred to as 0 eccentricity. Pressure was then applied at a constant rate until the leaf/runner assembly closed down to the base plate, i.e. 'rotor'. The pressure was varied in increments of 5psi [0.3bar] to a maximum upstream pressure of 50psig [3.5barg] before decreasing the pressure and averaging the data at each pressure point. This procedure was repeated for a range of eccentricities from the intended design point by increasing or decreasing the radial distance between the runner and base plate at cold conditions.

V. Results

The initial test at the design clearance of 0.120" [3.5mm] or 0 eccentricity highlighted stable operation of the leaves. The closure event did not show any signs of instability and the seal remained stable throughout the duration of testing.

The proximity probes captured the final stages of the closure event (Figure 11) before reliable film riding was achieved at approximately 20psig [1.4barg] upstream pressure and maintaining a constant gap between 0.005-0.010" [0.13-0.25mm] up to 50psig [3.5barg] with little hysteresis when removing the pressure. The full closure event was not captured as the cold build clearance was outside the range of the proximity probes and low speed data logging was in operation for prolonged testing.

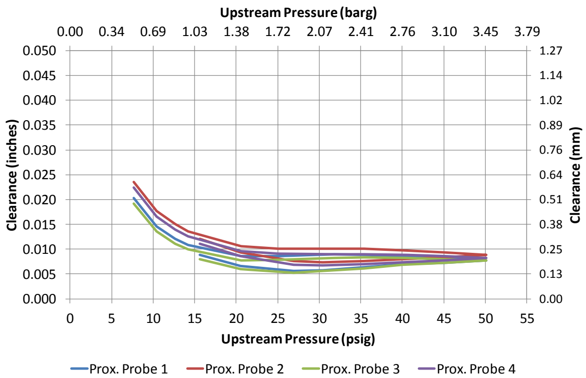

Figure 11:Runner Clearance vs. Upstream Pressures for the Zero Eccentricity

The pressure distribution under the runner can be seen in Figure 12 and Figure 13. Figure 12 shows the linear relationship of the pressure under the runner at each location relative to the upstream pressure. It is noted that P1 to P4 are the pressures under the clearance step and are seen to be very similar in value and are overlaid on the chart. P5 to P7 are pressures under the Rayleigh step and are lower than that of the clearance step, but again are similar in value to each other and are overlaid on the chart. Finally P8 to P14 are the pressures under the film riding surface and can be seen to be decreasing non-linearly with axial length. The pressure distribution from front to back can be seen in Figure 13. This shows the negligible drop in pressure from the upstream pressure (PFEED) to P4. A drop of approximately 2psi [0.14bar] can be seen at the Rayleigh step at 40psi [2.76bar] upstream pressure. The pressure distribution across the axial length of the Rayleigh step remains constant with equal values in pressure for P5, P6 and P7. At the step from the Rayleigh step to the film riding surface, a larger pressure drop is seen of approximately 5psi [0.34bar] at 40spi [2.76bar] upstream pressure. The pressure across the axial length of the film riding surface is of non-linear distribution to a downstream pressure of atmospheric conditions.

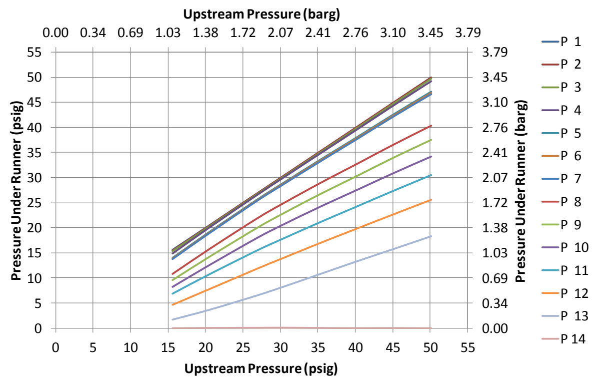

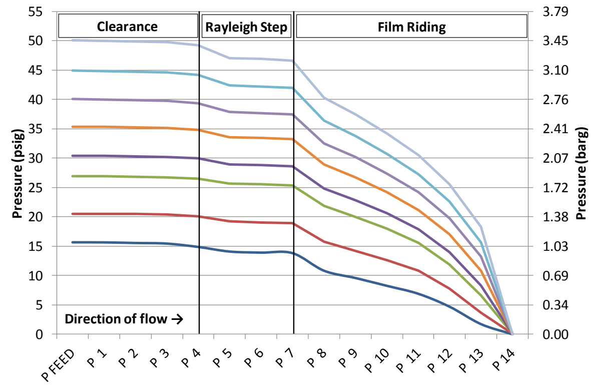

Figure 12: Film Pressure vs. Upstream Pressures for Each Pressure Tapping

Figure 13: Pressure Distribution Across the Runner for Various Upstream Pressures

Supplementary to the pressure sweep at the design clearance of 0.120" [3.05mm], the eccentricity was also examined. The analytical design, described earlier in the paper, predicted the average clearance of the runner at a range of eccentricity values for an upstream pressure of 40psig [2.76barg]. The test results have been plotted with the analytical results in Figure 14, where a negative eccentricity represents a larger radial gap between seal and rotor. The results show good correlation, validating CFD and FEM models. Full pressure sweeps were undertaken at all eccentricities during the testing and can be seen in Figure 15. Upstream pressures below 20psig [1.38barg] do not follow the trend of those above this value due the seal being in the process of closure at these pressures and obscuring the results. The results for 20-50psig [1.38-3.45barg] are similar in value for eccentricities from the design point to greater clearances. However, for greater interferences the gap increases with pressure with a total increase in gap from 20-50psig [1.38-3.45barg] of approximately 0.005"[0.13mm].

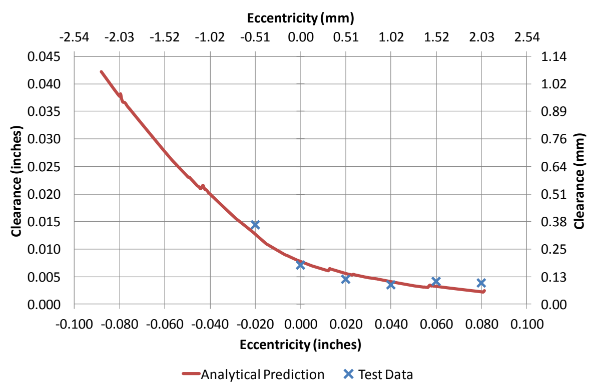

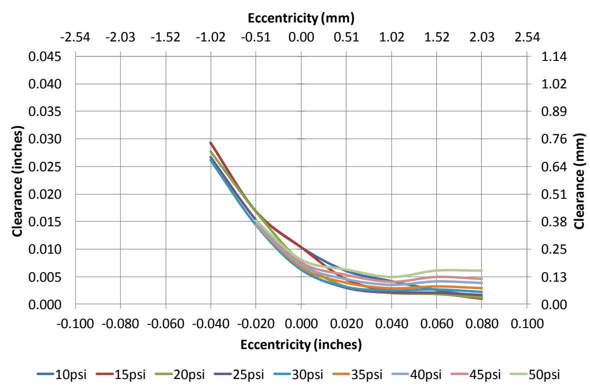

Figure 14: Clearance Predictions Compared with Actual Test Data at 40psi Upstream Pressure for Various Eccentricities

Figure 15: Clearance Test Data vs. Eccentricity for various Upstream Pressure Conditions

VI. Uncertainty Examination

The analytical design process took into consideration the tilt of the runner from front to back (Figure 16) and offered the optimum design for testing. This tilt was monitored throughout the testing using the proximity probes. An average angle of tilt can be seen in Figure 17 and Figure 18 over the range of pressures and eccentricities examined in this test program. The maximum angle of tilt is up to 0.16 degrees at an eccentricity of 0.060" [1.52mm] and an upstream pressure of 50psig [3.79barg]. The values for tilt throughout the testing remain positive indicating that the rear edge of the runner is lower than the front edge. The tilt appears to be dependent on both eccentricity and pressure with a convergence of angle at between 0-0.02" [0-0.51mm] eccentricity (Figure 17) and a decreasing angle with pressure for 0 eccentricity (Figure 18).

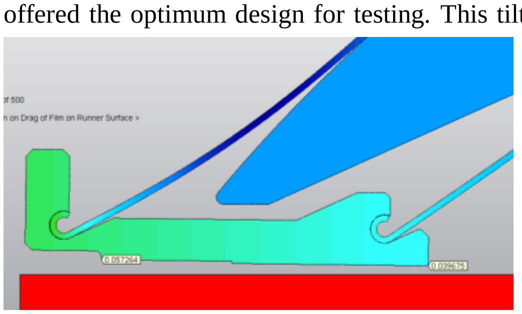

Figure 16: FEM Model Showing Runner Tilt

The rock of the runner was also examined in the testing, where rock was the average angle of the runner from left to right. The results can be seen in Figure 19 and Figure 20 with a maximum angle of no more than 0.07 degrees. The results are inconclusive to determine if eccentricity or pressure is a direct cause of rock.

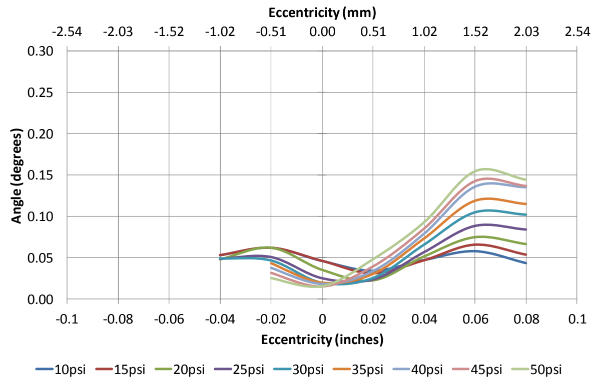

Figure 17: Runner Tilt Relative to Eccentricity

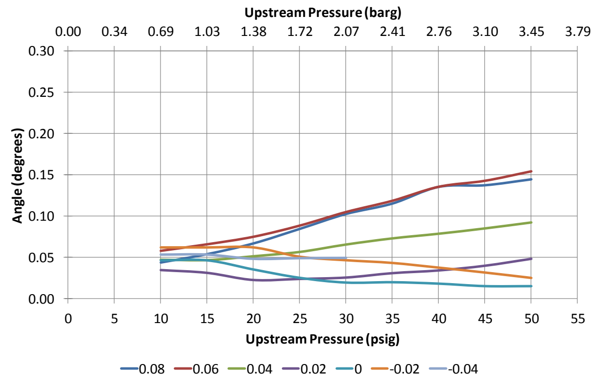

Figure 18: Runner Tilt Relative to Upstream Pressure

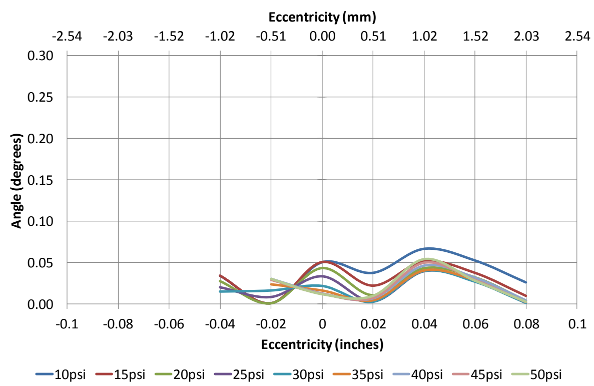

Figure 19: Runner Rock Relative to Eccentricity

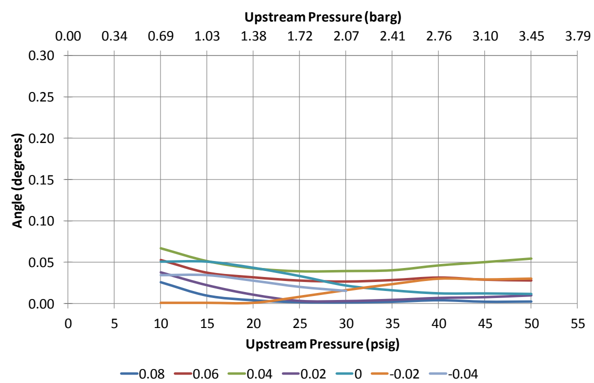

Figure 20: Runner Rock Relative to Upstream Pressure

Finally an attempt was made to manually excite the seal and investigate the effects of resonance. A 0.050" [1.27mm] shim was placed under the runner. A Pressure of 25psi was applied to insure the runner had fully closed to the shim. The shim was then quickly removed from under the runner and high speed data acquisition was used to log the gap from the proximity probes in conjunction with high speed photography to capture the effects. The test failed to destabilize the seal and within 11 oscillations at approximately 83Hz, the seal had stabilized back to the film riding condition. The average gap over time can be seen in Figure 21with points marked cross referencing the image taken through the viewing window by the high speed photography shown in Figure 22.

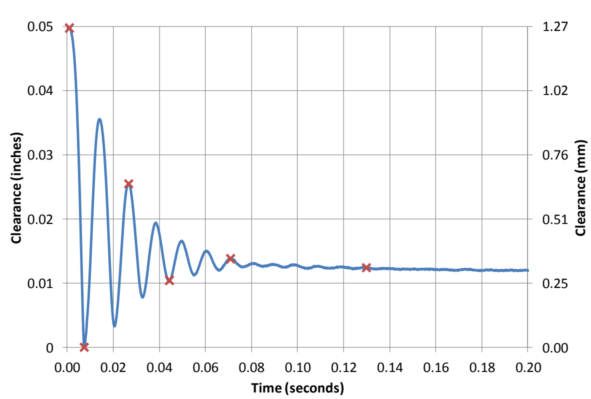

Figure 21: Gap Results for Manual Resonance Test

Figure 22: High Speed Images at Points Indicated in Figure 21 of Runner Relative to Base Plate

VII. Future Development

An advance program investigating the stability of the FRPALS is currently being undertaken by Bath University Department of Mechanical Engineering. A full size complete seal is being manufactured by Cross Manufacturing and supplied to Bath University for a 3 year test program including the design and development of a new dynamic test rig (Figure 23). The FRPALS design will be of reverse orientation with the leaves angled in the direction of flow (Figure 24). Analytical data shows the reverse design will result in a more compact design, offering the seal to a wider range of applications. The test rig will incorporate a vibration generator to investigate the dynamic stability including rotor dynamic coefficients, eccentric positioning between the rotor and stator and real engine run out simulation at speeds up to 654.5 ft/s [199.5 m/s], pressure drops up to 50 psi [3.5 bar] and frequencies up to 200Hz.

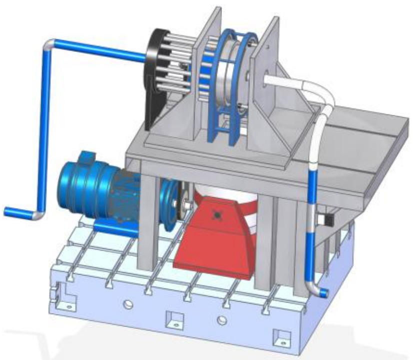

Figure 23: Test Rig Concept Courtesy of Bath University

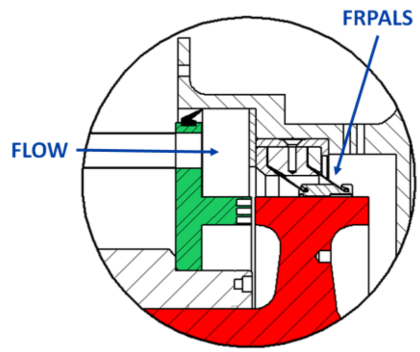

Figure 24: Cross Section of Test Rig Illustrating Reverse Design

VIII. Conclusion

Bench testing, analytical modeling and large application scale testing have all combined to prove the concept of the FRPALS. A design process has been developed that uses quick bench testing to validate analytical models used to acquire the optimum geometry for a sealing specification. This method along with the film riding concept has been validated against using large scale rig test data.

The FRPALS proved to be effective in a range of conditions and not only worked well at the design point, but showed capability to perform effectively at various eccentricities and over a wide range of pressure. The testing to date has not shown any signs of resonance or stability issues, but further investigation into these areas is planned for the future.

Acknowledgments

The authors would like to thanks the Directors of **Cross Manufacturing** for funding this work and allowing its publication. They would also like to thank their undergraduate placement student, Michael Dobson, for his outstanding effort in testing and data manipulation.

NYSERDA, New York State Energy Research and Development Authority, is acknowledged for work sponsored under Agreement No. 9887 that is background to the material presented. The opinions expressed in this report do not necessarily reflect those of NYSERDA or the State of New York.

References

[1]Grondahl, C. M., and Dudley, J. C., "Film Riding Leaf Seals for Improved Shaft Sealing" ASME Turbo Expo 2010, GT2010-23629, Vol. 4 Heat Transfer: Part A and B, Glasgow, UK, pp. 1293-1300

[2]Crudgington, P. F., Cross, R., Cross, E., "A Novel High Temperature Non-Contact Dynamic Seal" AIAA 2012-4004, 2004

[3]Bidkar, R. A., Ruggiero, E., J., and Wolfe, C., E., "Design and Testing Methodology for Motion & Vibration Characterization of Advanced Seals" AIAA 2011-5561, 2011

[4]Grodahl, C. M., Smith, R. L., Dudley, J. C., CMG Tech LLC, Rexford, NY, U.S. Patent "Film Riding Pressure Activated Leaf Seal Assembly," Patent No. US 8,474,827 B2, Jul. 2, 2013

[5]Justak, J. F., Advanced Technologies Group Inc, Sturat, FL, U.S. Patent "Non-Contact Seal for Gas Turbine Engine," Patent No. US 8,172,232 B2, May 8, 2012

[6]Bidkar, R. A., et al, General Electric Company, Niskayuna, NY, U.S. Patent "Film Riding Seal Assembly for Turbomachinery," Patent No. US 9,359,908 B2, Jun 7, 2016
[7]Bowsher, A., et al, "Pressure Activated Leaf Seal Technology Readiness," ASME Turbo Expo 2014, GT2014-27046, J. Eng. Gas Turbines Power 137(6), Jun 01, 2015
[8]Crudgington, P. F., "Recent Brush Seal and Testing Development at Cross" AIAA 2001-3480, 2001